

## HIGH-PRECISION BAYESIAN MODELING OF SAMPLES SUSCEPTIBLE TO INBUILT AGE

M W Dee<sup>1</sup> • C Bronk Ramsey

RLAHA, University of Oxford, Oxford OX1 3QY, United Kingdom.

**ABSTRACT.** Radiocarbon dates on samples susceptible to inbuilt age are common in the chronological record of many archaeological and environmental sites. Indeed, fragments of charcoal and wood are sometimes the only materials sufficiently well preserved for dating. However, where high-precision estimates are required the extra uncertainty associated with such measurements often renders them unusable. This article tests three Bayesian modeling approaches that are designed to tackle this problem. The findings of our study suggest that successful corrections can be made for the inherent age offsets. The most effective and versatile approach was based on a version of outlier analysis. It is hoped that this method will become more widely employed and enable samples susceptible to inbuilt age to be included in high-precision chronologies.

### INTRODUCTION

Selecting samples for radiocarbon dating involves an assessment of both context and material type (see Waterbolk 1971). Sometimes, however, the only materials available for dating are those susceptible to inbuilt age (IA). Fragments of charcoal, for example, are often more durable and in the soil than shorter-lived species like seeds, grasses, soft tissue, and bone. As a result, charcoal samples dominate the <sup>14</sup>C record for many sites. Furthermore, the magnitude of the IA associated with individual samples is often inestimable. Even if variables like the lifespan of the plant are taken into account, additional age from storage or reuse often remains indeterminable (see McFadgen 1982; Dee et al. 2009). For pre-Holocene sites, where the problem is usually encompassed by the uncertainty quoted in the date, the issue is of little significance. However, for late prehistoric and early historical sites where subcentennial precision is often demanded, a standardized and reliable correction for the problem would be of considerable value.

In this study, samples susceptible to inbuilt age (IA samples) are defined to be wood from inner tree rings, charcoal, or shell. In any other cases where the material being dated is likely to have been reused, the IA attribution may also apply. Various methods have been proposed for including IA samples in Bayesian models. Most advise treating the dates as *termini post quos* (TPQs, see Bayliss et al. 2012). Here, they just inform the algorithm that the date they offer must be older than context in which they were found. However, in models that also include dates on short-lived materials, such samples tend to add little value to the overall analysis, and where the model consists exclusively of IA samples, it seldom produces high-precision results. However, it is possible to reason that groups of samples susceptible to IA inherently contain more information than is represented by the use of TPQ commands. Indeed, methods have been designed that attempt to use such information to correct for any bias in the data. The principal assumption shared by these approaches is that the distribution of material ages in any group of IA samples can be modeled using an exponential curve. This does not mean the range of ages needs to precisely adhere to an exponential distribution. Instead, it postulates that if an infinite number of results were available on the context being dated, the corresponding age-density relationship is likely to be exponential in nature. Or, in more practical terms, most of the samples are likely to be close in age to the date being sought, with a diminishing number representing older and older material. The exponential relationship is not employed arbitrarily. Nicholls and Jones (2001) were the first to propose that IA samples could be represented by an exponential probability density related to the lifespan and growth habit of the antecedent trees. Intuitively, if the entire quantity of wood in an individual tree, or a collection of trees, were separated by age, the outer rings of the trunk and all the younger wood of the branches

---

1. Corresponding author. Email: michael.dee@rlaha.ox.ac.uk.

would exponentially outweigh the oldest heartwood. Further, in many cases where a specific event is being dated, such as the age of a hearth or the closure of a tomb, it is reasonable to assume that most of the material would be similar in age to the event, with a diminishing amount being considerably older. An obvious exception to this pattern arises where all the samples are significantly older than the event in question, as a result of practices like recycling or reclamation. This complication can be mitigated by including in the model short-lived samples, which can take the place of the missing younger material. Alternatively, a different relationship such as a Gaussian distribution may be appropriate. However, it is the opinion of the authors that such an occurrence, where practically none of the material dates to the same age as the event itself, would be extremely uncommon.

This article seeks to compare and evaluate three of the most common methods for modeling IA samples, using both theoretical and real-life examples. In each case, groups of IA dates are modeled and the results compared with dates that are either exactly known or can be independently verified. Variations of many of the modeling approaches described are available in other applications (see BCal, Buck et al. 1999; DateLab, Jones and Nicholls 2002), but the examples given here use OxCal (see Bronk Ramsey 1995, 2009) because that is the program with which the authors are most familiar.

## METHODS

### Modeling Approaches

#### 1. *Termini Post Quos (Afters)*

The most common method for modeling dates on IA samples is to enter them as TPQs. In OxCal, this is achieved by way of the After function. It employs a prior that only allows solutions to be drawn for the associated parameter that are from the younger end of the likelihood or younger still. As an example, the following code is used to define <sup>14</sup>C date “A” (3000 ± 30 BP) as a TPQ:

```
After()
{
  R_Date("A", 3000, 30);
};
```

#### 2. *Exponential Phase (Exp Phase)*

The Exponential Phase (Exp Phase) model treats a group of <sup>14</sup>C dates as if they represent a phase of activity that is exponential in shape. That is to say, it assumes the density of the results is likely to be greatest toward the younger end of the phase. Accordingly, the iterative process is exponentially biased toward solutions from the younger end of the phase. The Exp Phase is coded into OxCal using the Tau\_Boundary:

```
Sequence()
{
  Tau_Boundary();
  Phase()
  {
    R_Date("A", 3000, 30);
    R_Date("B", 3100, 30);
    R_Date("C", 3200, 30);
  };
  Boundary();
};
```

### 3. Exponential Outlier (Charcoal)

The Exponential Outlier method (Bronk Ramsey 2009) presupposes that all dates on IA samples can be treated as outliers. Here, as the model is calculated, a shift is applied to each solution drawn. The shift is always toward younger ages and its value is randomly selected from an exponential probability density function, whose parameters can either be specified in advance or estimated by the model itself. In the latter (default) scenario, the function automatically scales to fit the spread of the dates in the phase. Significantly, the scaling of the exponential prior is logarithmic with respect to absolute time. That is to say, an exponential function with 10 yr as its time constant is equally likely to one with 100 yr. This is not the case with the Exp Phase prior, where every calendar year is equally likely. To employ the Exponential Outlier (henceforth, “Charcoal”) approach in OxCal, the following code is required:

```
Outlier_Model("Charcoal", Exp(1, -10, 0), U(0, 3), "t");
```

In addition, every IA sample in the model must be labeled and “tagged” with an outlier probability equal to 1:

```
R_Date("A", 3000, 30)
{
  Outlier("Charcoal", 1);
};
```

## TYPES OF EVENT ESTIMATION

Two different types of event estimation were addressed in this study. The first, denoted single event estimation (SEE), arises where a date is sought for an individual event in the past. Here, any variation in the data set, with the exception of measurement scatter, comes *solely* from inbuilt age because each of the samples relates directly to the same event. Examples might include the completion date of a timber structure or a charcoal deposit from a destruction layer. The second type is defined as phase boundary estimation (PBE). This is where a date is sought for the transition point between two or more phases in the archaeological or environmental record. In this case, the dates themselves are naturally spread across the duration of each phase, but each one *additionally* contains inbuilt age. Examples of this kind are ubiquitous and include all charcoal and wood samples from phases ordered by relative methods such as stratigraphy or typological sequences.

### Single Event Estimation (SEE)

Determining the precise date of an individual event in the past is one of the most common objectives of chronology. In  $^{14}\text{C}$  dating, the simplest approach involves combining multiple measurements on annual samples that emanate precisely from the year in question. Examples might include measurements on commemorative bouquets or well-contextualized seeds. However, even if their connection with an event is unequivocal, longer-lived materials invariably return  $^{14}\text{C}$  dates that are too old. In order to assess how well the three modeling approaches introduced above counteract this effect, the following theoretical and actual case studies were employed.

#### 1. Theoretical SEE

Sets of 20  $^{14}\text{C}$  dates were simulated for the arbitrarily chosen calendar date of 2000 BCE (3950 BP) using the `R_Simulate` function in OxCal. In the Control case, the dates were treated as if they came from annual samples, such as grasses or seeds. In the remaining scenarios, the dates were artificially subjected to IA, which was simulated exponentially, resulting in most samples being only slightly older than 2000 BCE but a few being considerably greater in age. The exact IA added to

each date was obtained by random selection from an exponential probability density function (see code below) and the severity of the issue was varied by using three different time constants ( $\tau$ ):

Table 1 The OxCal code was used to artificially age each date.

Data set	$\tau$ (calendar years)	OxCal code (for Date "1")
Control	0	<code>R_Simulate("1", 3950, 30);</code>
1a	50	<code>R_Simulate("1", 3950-50*ln(rand()), 30);</code>
1b	100	<code>R_Simulate("1", 3950-100*ln(rand()), 30);</code>
1c	200	<code>R_Simulate("1", 3950-200*ln(rand()), 30);</code>

Calibrated date ranges for the Theoretical SEE Control and IA data sets 1a–1c are given in Table S1 in the Supplemental Online Material (SOM). As evident in Figure 1, the average calendar dates from the “artificially aged” data were indeed approximately exponentially distributed in absolute time.

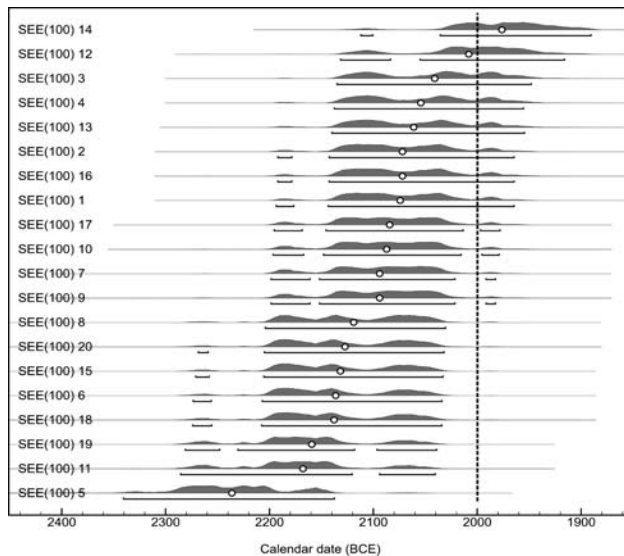


Figure 1 Data set 1b for theoretical SEE modeling. The data was subjected to an exponential bias with  $\tau = 100$  yr. The average calendar date is represented by the dot at the center of the 95% calendar date ranges. The true age is exactly 2000 BCE (dashed line).

The Control data set was averaged using the `R_Combine` function in OxCal. This provided what would be a typical  $^{14}\text{C}$  estimate for the true date of the context if the samples had not been IA samples, e.g. short-lived plants. The 1a–1c calibrations were extracted as prior distributions so the three modeling approaches (Afters, Exp Phase, and Charcoal) could be applied to them equally and independently. In the resulting models, the simulated dates were grouped into phases and the end boundaries of the phases taken to represent the corrected date. The basic code for the theoretical SEE models is given in the SOM.

## 2. Actual SEE

### *The Pyramid of Khafre, Giza*

Bonani et al. (2001) published 25  $^{14}\text{C}$  dates on the Pyramid of Khafre, Giza. All the samples were made on charcoal inclusions in the mortar (Bonani et al. 2001; Dee et al. 2009). The dates are republished in Table S2 in the SOM. As is evident in Figure 2, however, the data set presents an archetypical example of a suite of samples susceptible to IA that collectively approximates an exponential curve.

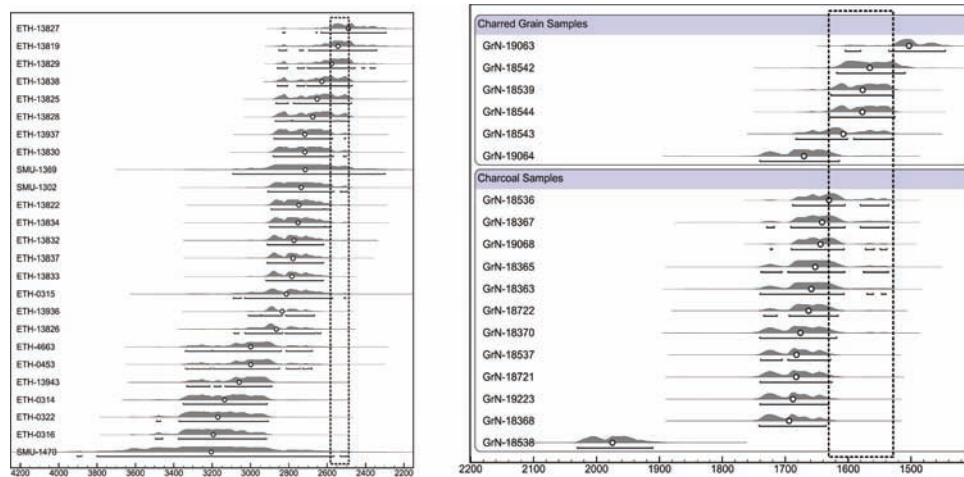


Figure 2 Radiocarbon dates for the pyramid of Khafre (left, Bonani et al. 2001) and the destruction of Jericho (right, Bruins and van der Plicht 1995). The average calendar date is represented by the dot at the center of the calendar date ranges (95%). The estimated true age for the pyramid of Khafre was obtained from historical records (2537 BCE, Kitchen 2000) and includes the 100-yr uncertainty suggested by Kitchen (1991); the estimated true age for the destruction of Jericho was obtained by averaging the short-lived plant results (1634–1529 BCE, 95%).

New estimates were produced for the completion date of the pyramid using the three different modeling approaches described above. As in the theoretical case, the end boundaries from the three models were taken to represent the corrected date. A historically derived date for the pyramid's completion (the accession of his successor) was also included as an approximate "true age." The OxCal code for the models is given in the SOM.

#### *The Middle Bronze Age Destruction of Jericho (Tell es-Sultan)*

Bruins and van der Plicht (1995) published a set of 12  $^{14}\text{C}$  dates on charcoal from a Middle Bronze Age destruction layer at Jericho (see Table S2, SOM). In this case, most of the results clustered together; however, they also clearly contained IA because 6 concurrently measured short-lived grain samples returned much younger dates. Together, the overall spread of ages was approximately exponential (see Figure 2). An estimate of the true age of the stratum was obtained by using the `R_Combine` function on the grain samples.<sup>2</sup>

The methods for modeling IA samples were then applied to the data set as a whole, although slight adjustments had to be made to the Afters and Charcoal models to allow for the grain samples. Specifically, this meant not regarding them as TPQs in the former case, and treating them as General outliers in the latter. The General Outlier model can be employed in tandem with the Charcoal Outlier model, wherein it operates solely on the dates labeled "General." It also employs random shifts, but this time from a Student's  $t$  distribution [ $t(5)$  or in OxCal  $T(5)$ ], so they may be to either younger or older ages (see Bronk Ramsey 2009). Due to their improved reliability, General dates are usually only given a 5% outlier probability. Once more, the OxCal code for each model is given in the SOM.

#### **Phase Boundary Estimation (PBE)**

Dates for the transition point between two phases of cultural or environmental activity are frequently sought by chronologists (Buck et al. 1992; Bronk Ramsey 1995; Nicholls and Jones 2001). Where

2. The weighted average of all 6 grain samples failed the Ward and Wilson (1978) test ( $t = 24.1$  versus 11.1;  $df = 5$ ), so the date with the highest  $t$  statistic was removed (GrN-19063) and the average recalculated.

short-lived material is available for each phase, Bayesian models usually apply the assumption of a uniform probability density (Buck et al. 1991). That is to say, any sample is equally likely to come from any calendar year of the phase. Indeed, it is also assumed all possible phase lengths are equally probable (Nicholls and Jones 2001). However, difficulties arise when the datable materials are likely to contain IA. Such samples might artificially extend the phase to which they belong, which in turn could distort the position of other phases in the model.

Dates in phases are usually more widely dispersed than is the case for single events. However, IA still often biases the data in an exponential fashion. Accordingly, PBE and SEE models are calculated in exactly the same way. In fact, the latter can just be considered a special case of the former, where the true age being modeled relates to a phase of just 1 yr. For PBE, the ordering of all the phases in the sequence is a pivotal factor in combating IA. In some cases, short-lived species may help to securely anchor one or more phases in the sequence. In order to assess how well the three modeling approaches counteract the effect of IA within phases, the following theoretical and actual case studies were examined.

### 1. Theoretical PBE

Sets of 20  $^{14}\text{C}$  dates were simulated for the period 2000–2200 BCE (3950–4150 BP) using the `R_Simulate` function in OxCal. Simulations were made every 10 calendar years and formed two phases of 10 dates: 2205–2095 and 2105–2195 BCE. Distributing the dates in this manner implied the correct date for the transition between the two phases was 2100 BCE. In the Theoretical PBE Control case, the dates were treated as if they came from annual samples. In the remaining scenarios (2a–2c), the dates were artificially subjected to IA. The inbuilt aging was simulated by using an exponential function in the same manner as for the Theoretical SEE. The obvious difference this time was that each date was not only subject to IA, but also had a different true age. Once again, the severity of the issue was varied by using three different time constants (2a,  $\tau = 50$ ; 2b,  $\tau = 100$ ; 2c,  $\tau = 200$ ). The calibrated date ranges for the Control and IA data sets 2a–2c are given in Table S3, SOM. Figure 3 shows the data ordered by age, confirming that they do indeed veer away from the true position of the phases in an exponential fashion.

The simulated calibrations for the Control data set were included in a simple two-phase sequence model. This provided a typical  $^{14}\text{C}$ -based estimate for the transitional boundary, if all the samples had been short lived. For data sets 2a–2c, the aged calibrations were extracted as prior distributions, so the three modeling approaches (Afters, Exp Phase, and Charcoal) could be applied to them equally and independently. The distributions were included in the simplest two-phase sequence models possible for each method. For the Afters model (2a), this meant applying the `After` command to each date, and for the Charcoal model, labeling them all as Charcoal outliers. However, the Exp Phase model had to be built in a slightly more convoluted fashion because two exponential phases cannot follow each other directly in a sequence. The basic code for the theoretical PBE models is given in the SOM.

### 2. Actual PBE

Of the various scenarios examined in this paper, actual phase boundary estimation is the most difficult to test. What is required is a series of contexts for which IA samples have been obtained that are also separated by boundaries of known age. As IA samples are usually considered a last resort for dating, their selection for contexts bound by well-dated transitions is very rare indeed. One of the best examples available comes again from the 4th Dynasty of ancient Egypt. By pooling the  $^{14}\text{C}$  dates published for the consecutive rulers Sneferu and Khufu (see Table 2 and Table S4, SOM), the three modeling approaches can be used to estimate the transition date between each



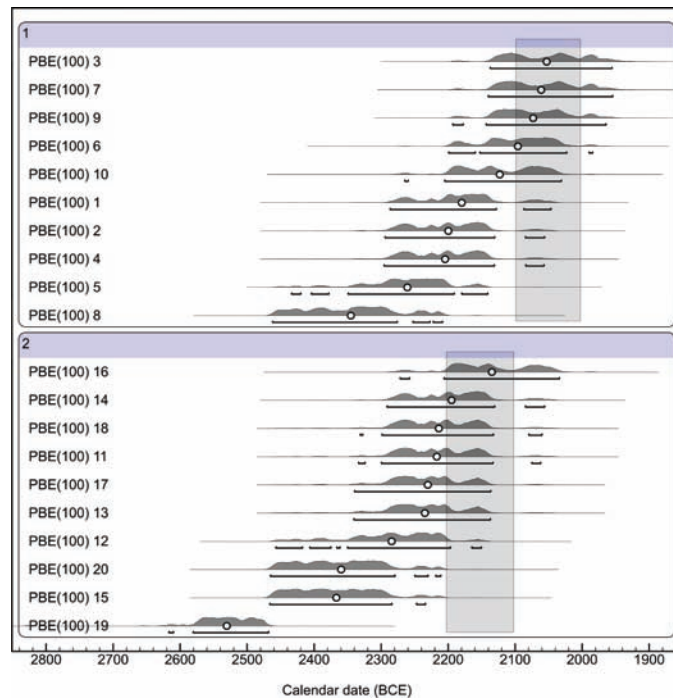


Figure 3 Data set 2b for theoretical PBE modeling (95% calibrations). Two 100-yr phases (gray rectangles) were prepared, which abutted at 2100 BCE. Dates were simulated at uniformly distributed points across each phase, and further age added by random sampling from an exponential distribution with  $\tau = 100$  yr.

reign; that is, the accession date of Khufu. The working assumption is that, because of the number of contexts involved and their magnitude, the samples are likely to have come from a number of different years of each reign. Further, because Khufu’s accession date has already been estimated on the basis of archaeological and textual evidence, there is independent information available to test the results. Furthermore, Bronk Ramsey et al. (2010) produced a probability density function for the accession date based on both historical evidence and an independent set of wholly short-lived samples.

Table 2 Published <sup>14</sup>C dates used for actual PBE modeling. The full list of dates, and the OxCal model code, is given in the SOM.

King	Context	Number of dates	Material	Reference
Sneferu	Pyramid, Meydum	9	Wood	Libby 1955; Agrawal and Kusunigar 1975; Bonani et al. 2001
	Bent Pyramid, Dahshur	5	Wood and charcoal	Ralph 1959; Barker et al. 1971; Bonani et al. 2001
	Tomb 17, Meydum	3	Grass	Bonani et al. 2001
Khufu	Funerary Boat, Giza	3	Wood and grass	Stuckenrath and Ralph 1965; Long 1976
	Great Pyramid, Giza	46	Charcoal and grass	Bonani et al. 2001

## RESULTS AND DISCUSSION

### Single Event Estimation (SEE)

#### 1. Theoretical SEE

The 9 corrected dates and the average obtained from the Control set are shown in Figure 4 and the data are provided in Table S1, SOM. The most conspicuous outcome of the SEE tests was how poorly the Afters model performed. In each of the three scenarios, the results it produced were both incorrect and markedly broader than the other two methods. The Charcoal model resulted in the most accurate estimates, providing probability density functions that overlapped with the target date (2000 BCE) in all cases. The Exp Phase model generated the most precise results, which were also quite accurate, although the output for the samples offset by an average of 100 yr (data set 1b) was slightly too old.

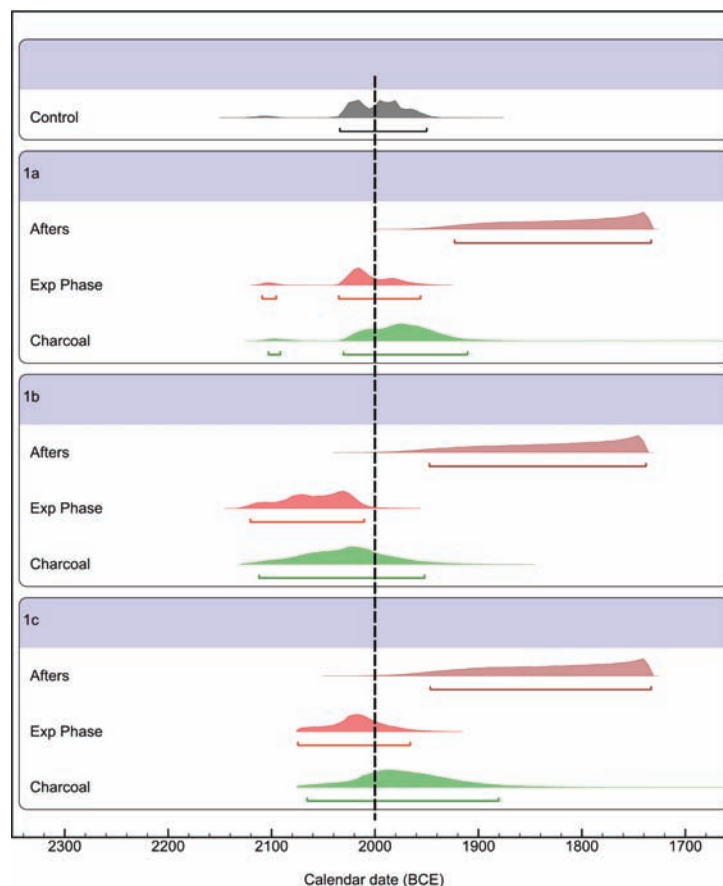


Figure 4 Corrected dates for data sets 1a–1c and the averaged result from the Control data set. The true age of 2000 BCE is indicated by the dashed line.

#### 2. Actual SEE

The corrected estimates for the completion of the pyramid of Khafre and the Middle Bronze Age destruction of Jericho are shown in Figure 5, and the data is given in Table S2, SOM. A historical date for the end of Khafre's reign (Kitchen 2000) and an average obtained on the short-lived grain samples from Jericho are included as approximate true ages. The likely uncertainty in the Khafre



date is taken from Kitchen (1991). As with the Theoretical SEE example, the Afters model for the Pyramid of Khafre generated a date that was not only too young but so imprecise as to be essentially meaningless. However, because the Jericho data set also included some short-lived samples, the same approach was more successful and produced results that overlapped the expected date range. For both contexts, the Charcoal and Exp Phase models produced results that agreed with the expected ages. Significantly, in the case of the destruction layer, the results obtained by including the charcoal samples were slightly more precise than those obtained by simply averaging the short-lived grain samples.

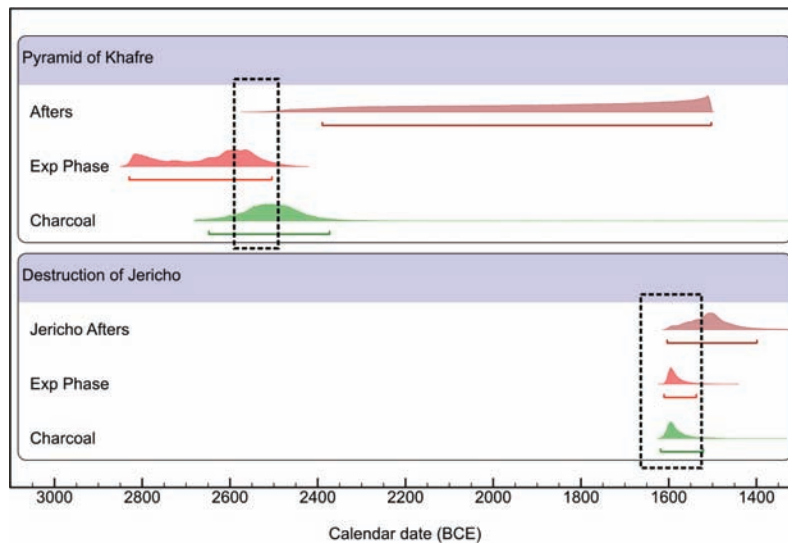


Figure 5 Corrected dates for the pyramid of Khafre and the Middle Bronze Age destruction of Jericho. The independently estimated true ages are shown by the dashed lines.

## Phase Boundary Estimation (PBE)

### 1. Theoretical PBE

The nine corrected phase boundary estimates and the average obtained from the control set are shown in Figure 6, and the data is given in Table S3, SOM. Unlike the SEE case, on this occasion the Afters model did agree with the known true age in two of the three cases. However, once more, in the absence of any short-lived material the resulting date was extremely broad. The other two approaches performed in much the same way as they had for the SEE case, with the Exp Phase models producing the most refined estimates, albeit erring towards older ages, and the Charcoal model generating calibrations that centered almost symmetrically about the target date (2100 BCE).

### 2. Actual PBE

The corrected estimates for the transition boundary between the reigns of Sneferu and Khufu are shown in Figure 7, and the data are given in Table S4, SOM. A historical date for Khufu's accession (Kitchen 2000), including the probable uncertainty in this date suggested by Kitchen (1991) and a <sup>14</sup>C-based estimate for the same event obtained on short-lived samples by Bronk Ramsey et al. (2010) are included as approximate true ages.

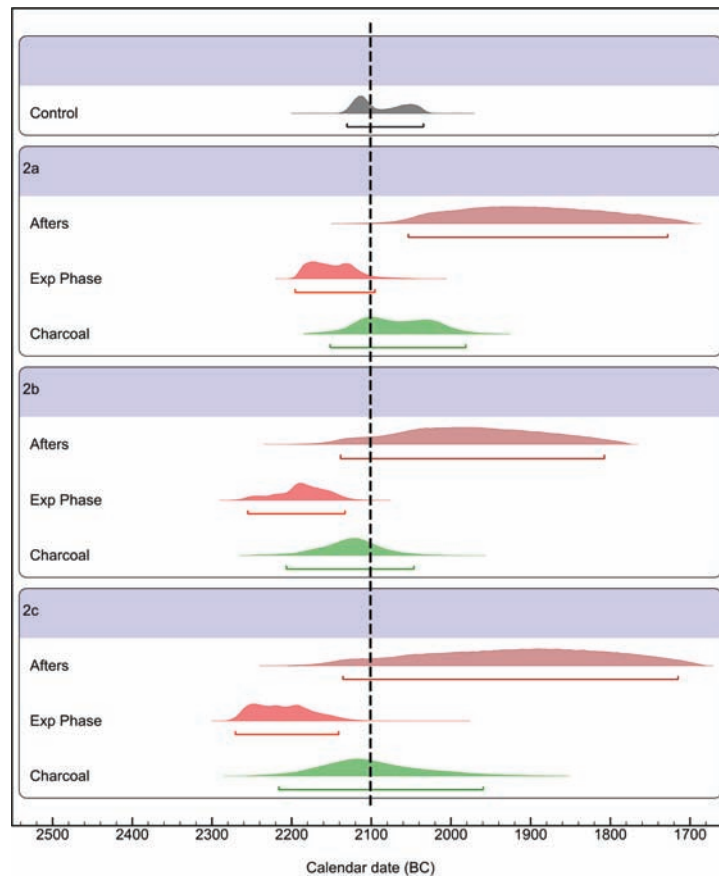


Figure 6 Corrected dates for data sets 2a–2c and the averaged result for the Control data set. The true age of 2100 BCE is indicated by the dashed line.

In the Actual PBE example, 5 of the 66 dates were made on short-lived samples. Because of this, the Afters model showed some improvement, producing a refined calibration that was only slightly younger than the expected age. On the other hand, the Exp Phase model performed poorly. In fact, it failed to run several times and the eventual result should be considered unreliable because of its overall Agreement Index (~10%, see Bronk Ramsey 1995). The Charcoal model produced a probability density function that was consistent with Kitchen's (2000) historical estimate, and overlapped with the range generated by Bronk Ramsey et al. (2010). Significantly, however, the Charcoal estimate tended toward younger ages than the 2010 analysis on short-lived plants. This finding may be real, and the study of Bronk Ramsey et al. (2010), which was deficient in samples around this period, may indeed be slightly too old. However, the situation also hints at a complication that would not have existed in the theoretical case; namely, where some of the IA samples are younger than the context they represent. Fortunately, a bespoke version of the Charcoal model can be applied in cases where such outliers are suspected. Here, the standard exponential shape is modified to provide a minute level of probability for the presence of intrusive material. This model, referred to as the Charcoal Plus, takes the shape given in Figure 8 and is scalable in the normal manner (see Bronk Ramsey 2009). The data for the Charcoal Plus model is given in the SOM and its output when applied to the Sneferu and Khufu data is included in Figure 7.

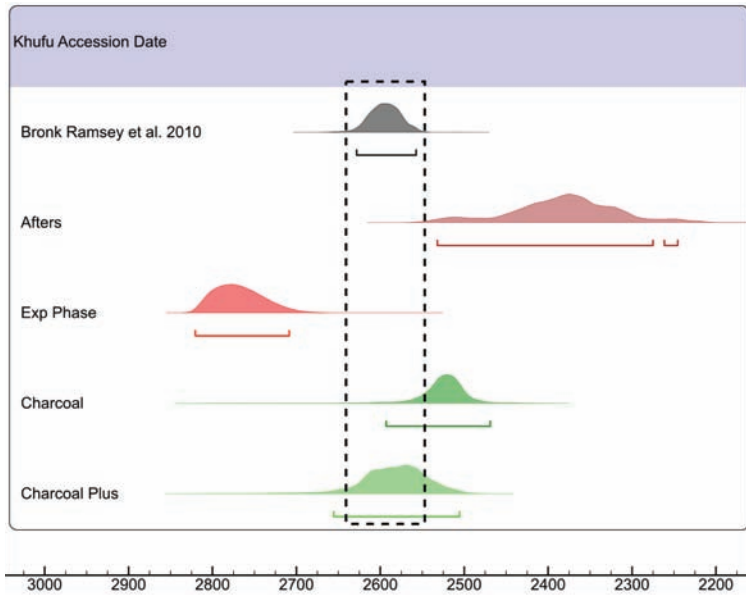


Figure 7 Corrected dates for the accession of king Khufu of Egypt. The independent age estimates were taken from a historical source (2593 BCE, Kitchen 2000) and a <sup>14</sup>C-based estimate made by Bronk Ramsey et al. (2010) on a separate set of short-lived plant samples (2629–2558 BCE).

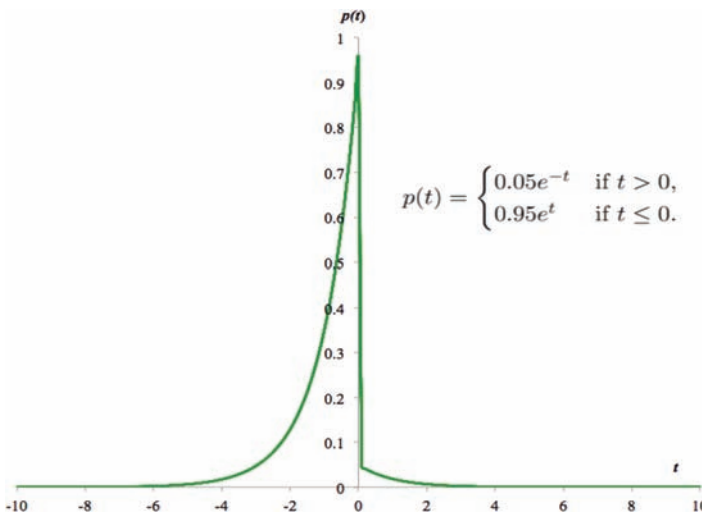


Figure 8 Probability density function used for the Charcoal Plus model. In cases where a small number of young outliers may be present amid the IA samples, this scalable function may be more appropriate than the standard Charcoal model. Note:  $t$  is not time strictly speaking, as the Charcoal Plus model is scaled during calculation  $-t$  is a factor in the time.

**CONCLUSIONS**

In many instances, the only material available for <sup>14</sup>C dating is tainted by the problem of IA. Doubts over the accuracy of such samples compromises their application to high-precision work. As a result, large numbers of dates on IA samples languish unused in the published literature. However, as the number of results for a given context increases, there is a concordant improvement in the likelihood that its true age can be reliably estimated. The assumption most commonly employed is that the results will cluster close to the true age of the event, with a small proportion reflecting a greater degree of IA. This article tested various Bayesian modeling approaches that use such patterning to combat IA. In both the theoretical and actual cases, the following three conclusions were strongly supported. Firstly, methods employing the assumption of an exponential distribution of IA

samples over time do generate reliable results. Hence, the common belief that samples susceptible to IA should only be treated as *termini post quos* seems to be too conservative. In fact, if no more precise dating information is available, it has been shown here that treating dates on IA samples as TPQs can lead to spurious results. Secondly, the Charcoal model, developed from outlier analysis, most accurately corrected the various data sets. Indeed, in every example tested, the 95% probability range produced by the Charcoal model encompassed the known true date. Finally, in real-world situations where the sample set is not only affected by IA, but also potentially by intrusive material, the subtly modified Charcoal Plus model is recommended.

## REFERENCES

- Agrawal DP, Kusumgar S. 1975. Tata Institute radiocarbon date list XI. *Radiocarbon* 17(2):219–25.
- Barker H, Burleigh R, Meeks N. 1971. British Museum natural radiocarbon measurements VII. *Radiocarbon* 13(2):157–88.
- Bayliss A, van der Plicht J, Bronk Ramsey C, McCormac G, Healy F, Whittle A. 2012. Towards generational time-scales: the qualitative interpretation of archaeological chronologies. In: Whittle A, Healy F, Bayliss A, editors. *Gathering Time*. Oxford: Oxbow. p 17–59.
- Bonani G, Hass H, Hawass Z, Lehner M, Nakhla S, Nolan J, Wenke R, Wölfli W. 2001. Radiocarbon dates of Old and Middle Kingdom monuments in Egypt. *Radiocarbon* 43(3):1297–320.
- Bronk Ramsey C. 1995. Radiocarbon calibration and analysis of stratigraphy: the OxCal program. *Radiocarbon* 37(2):425–30.
- Bronk Ramsey C. 2009. Dealing with outliers and offsets in radiocarbon dating. *Radiocarbon* 51(3):1023–45.
- Bronk Ramsey C, Dee M, Rowland J, Higham T, Harris S, Brock F, Quiles A, Wild E, Marcus E, Shortland A. 2010. Radiocarbon-based chronology for dynastic Egypt. *Science* 328(6154):1554–7.
- Bruins HJ, van der Plicht J. 1995. Tell es-Sultan (Jericho): radiocarbon results of short-lived cereal and multiyear charcoal samples from the end of the Middle Bronze Age. *Radiocarbon* 37(2):213–20.
- Buck CE, Litton CD, Smith AFM. 1991. Calibration of radiocarbon results pertaining to related archaeological events. *Journal of Archaeological Science* 19(5):497–512.
- Buck CE, Kenworthy JB, Litton CD, Smith AFM. 1992. Combining archaeological and radiocarbon information: a Bayesian approach to calibration. *Antiquity* 65(249):808–21.
- Buck CE, Christen JA, James GN. 1999. BCAL: an online Bayesian radiocarbon calibration tool. *Internet Archaeology* 7. <http://dx.doi.org/10.11141/ia.7.1>.
- Dee MW, Bronk Ramsey C, Shortland AJ, Higham TFG, Rowland JM. 2009. Reanalysis of the chronological discrepancies obtained by the Old and Middle Kingdom Monuments Project. *Radiocarbon* 51(3):1061–70.
- Jones M, Nicholls G. 2002. New radiocarbon calibration software. *Radiocarbon* 44(3):663–74.
- Kitchen KA. 1991. The chronology of ancient Egypt. *World Archaeology* 23(2):201–8.
- Kitchen KA. 2000. Regnal and genealogical data of ancient Egypt (Absolute Chronology I) the historical chronology of ancient Egypt, a current assessment. In: Bietak M, editor. *The Synchronisation of Civilisations in the Eastern Mediterranean in the Second Millennium BC I*. Vienna: Austrian Academy of Sciences. p 39–52.
- Libby WF. 1955. *Radiocarbon Dating*. 2nd edition. Chicago: University of Chicago Press.
- Long RD. 1976. Ancient Egyptian chronology, radiocarbon dating and calibration. *Zeitschrift für Ägyptische Sprache und Altertumskunde* 103:30–48.
- Nicholls G, Jones M. 2001. Radiocarbon dating with temporal order constraints. *Applied Statistics* 50(4):503–21.
- McFadgen BG. 1982. Dating New Zealand archaeology by radiocarbon. *New Zealand Journal of Science* 25:379–92.
- Ralph EK. 1959. University of Pennsylvania radiocarbon dates III. *Radiocarbon* 1:45–58.
- Stuckenrath JR, Ralph EK. 1965. University of Pennsylvania radiocarbon dates VIII. *Radiocarbon* 7:187–99.
- Ward GK, Wilson SR. 1978. Procedures for comparing and combining radiocarbon age determinations: a critique. *Archaeometry* 20(1):19–39.
- Waterbolk HT. 1971. Working with radiocarbon dates. *Proceedings of the Prehistoric Society* 37:15–33.